

Measurements and Simulations of a 20 GHz Metamaterial Lens

Cassandra Whitton¹, Christopher Groppi², Philip Mauskopf³, Jose Siles⁴, and Adrian Tang⁵

Abstract—In this paper, we present measurements of a prototype metamaterial flat lens. Flat lenses with short focal lengths are interesting due to their potential use in remote sensing for both space-based cubesat applications and larger form factors. Our metamaterial flat lens was manufactured by using 11 layers of RO3003 circuit board laminate with etched sub-wavelength-sized copper patterning. The copper patterning is designed in such a way as to maximize the transmittance of the lens while applying the correct phase shift across the lens plane to give the lens gaussian focal properties. The lens was measured by scanning a receiver horn through one axis of the image plane of a transmitting horn. This measurement demonstrated that the waist of the focused gaussian beam is 30% wider than ideal. It is suspected that this non-ideality is caused by phase error in the design process. We have created an electromagnetic simulation based on Fourier optics which will soon be able to characterize such non-idealities. Further measurements will be useful to fully characterize the lens’s focal properties and determine how much loss it incurs.

I. INTRODUCTION

CubeSats are an attractive prospective for those wishing to perform terahertz observations in space, due to the high atmospheric attenuation at these frequencies which makes ground-based observing difficult or impossible [7], and due to the prohibitively high costs of larger satellites. However, CubeSat missions come with their own set of design challenges, which particularly includes the requirements for low weight and small form factor [3]. As a partial solution to this, using metamaterial lenses as primary observing apertures in such systems can help ameliorate some of these challenges.

Metamaterials, which often involve the structured embedding of metal elements within dielectric substrates, and metamaterial lenses in particular, have recently seen much advancement and development into the millimeter wavelength regime [4], [5]. The lenses which have been created so far are both thin and lightweight compared to a conventional lens of equivalent f -number, freeing up weight budget and making it easier to place and stow the lens, if a deployable design

is necessary or desirable. Furthermore, the design techniques introduced by Ref. [5] ensure that no anti-reflection coating is necessary to minimize reflection losses. Such lenses have been found to theoretically have less than half a dB of loss, which is significantly better than that of a Fresnel zone plate lens, which, while flat and light, can exhibit on the order of 3 to 4dB or more of loss [6].

Here we have created and tested a metamaterial flat lens which operates at 20 GHz. The lens we present here is intended to act as a low-frequency prototype to test our design procedure. We are also developing a complementary electromagnetic simulation to refine our design process and to more accurately determine the optical properties of our lenses before fabrication. A successful design procedure should allow us to experiment with more expensive high-frequency designs, operating at 600 GHz or even above 1 THz.

II. LENS DESIGN

The lens is designed to operate at 20GHz by transforming a plane wave (with a flat phase-front) to the phase of a converging gaussian beam. This phase transformation is approximated by Refs. [5] and [2] as

$$\phi(r) = -\frac{\pi r^2}{\lambda R} \quad (1)$$

where λ is the operational wavelength, r is the distance on the lens plane from the lens center, R is the radius of curvature of the phase front, given by

$$R(f) = f + \frac{\left(\frac{\pi w_0^2}{\lambda}\right)^2}{f} \quad (2)$$

and w_0 is the waist of the focused beam at the focal plane. The focal length of the lens is given by f .

In the case of our lens, the diameter of the active area is 254 mm, and the focal length is 105 mm, making our lens an $f/0.41$ lens. These design parameters result in the phase transformation shown in the top plot of Fig. 1.

Given this phase transformation, we grid the surface of the lens vertically and horizontally into pixels, each of square dimensions $\lambda/10$, or 1.50 mm. Each of these pixels is assigned a single phase transformation value based on the above equations. In our case, each pixel has 10 metal layers, with 10 copper squares of metal, stacked on top of each other and separated by 11 surrounding dielectric layers. The dimensions of each square may be picked freely. Then, using techniques as described in Ref. [5], each pixel is optimized to give the desired phase transformation and maximum transmittance. These optimizations work by automatically

Submitted for review 28 February 2021.

This work was supported in part by the JPL SURP program. RO3003 material used in this work was provided gratis by Rogers Corporation.

¹Cassandra Whitton is with the School of Earth and Space Exploration, Arizona State University, Tempe, AZ 85287, USA (e-mail: cassandra.whitton@gmail.com)

²Christopher Groppi is with the School of Earth and Space Exploration, Arizona State University, Tempe, AZ 85287, USA (e-mail: cgroppi@asu.edu)

³Philip Mauskopf is with the School of Earth and Space Exploration, Arizona State University, Tempe, AZ 85287, USA (e-mail: philip.mauskopf@asu.edu)

⁴Jose Siles is with the Jet Propulsion Laboratory, Pasadena, CA 91109, USA (e-mail: jose.v.siles@jpl.nasa.gov)

⁵Adrian Tang is with the Jet Propulsion Laboratory, Pasadena, CA 91109, USA (e-mail: adrian.j.tang@jpl.nasa.gov)

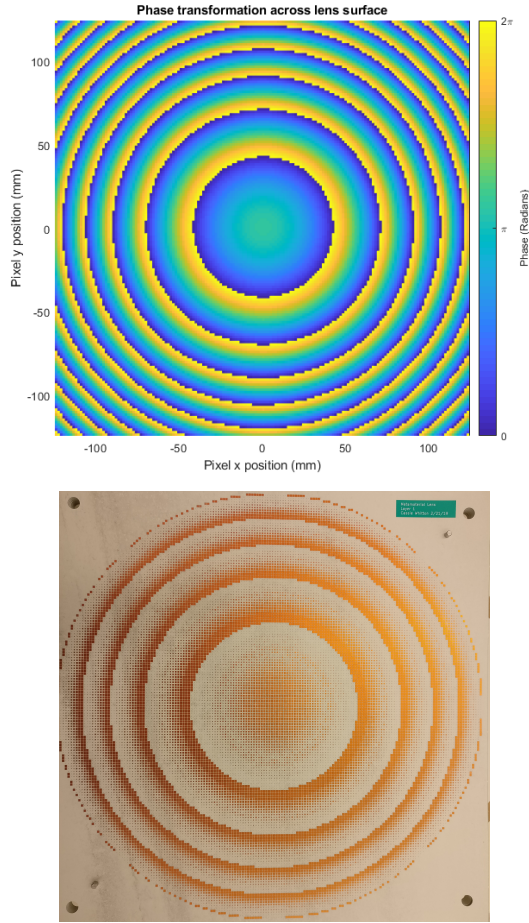


Fig. 1. The designed lens phase transformation (above) is compared with one layer of the manufactured lens (below). The layer’s pattern is made up of thousands of copper squares.

tweaking the dimensions of each metal square until the desired conditions for that pixel are met. Because each pixel is treated independently from each other pixel, this is relatively computationally simple, as it only requires the optimization of around 5 free parameters (one for each layer of the lens, divided by 2 due to symmetry across its center) per pixel.

The lens was manufactured on RO3003 circuit board laminate with 760 mm thickness, with 1 ounce copper cladding. Due to manufacturing tolerances, the metal squares were constrained to be no smaller than 200 μm in dimension, with at least 200 μm between adjacent squares. A single layer of the manufactured lens is shown in the bottom half of Fig. 1. The layers were then stacked together, as shown in Fig. 2, using alignment holes that were drilled into the laminate layers during manufacturing. The completed lens is roughly 0.59 cm thick.

Though not directly relevant to this experiment, the lens is designed in such a way that it may be scaled from 20 GHz to 600 GHz. In doing so, the layer thicknesses and metal square sizes would be reduced by a factor of 30. Though this places much stricter tolerances on the manufacturing process,

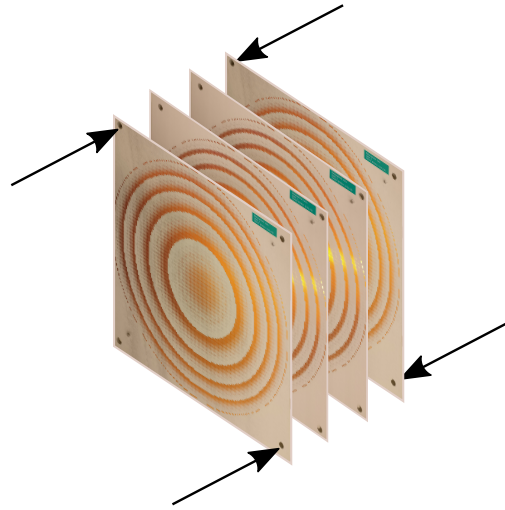


Fig. 2. Multiple layers of the lens are stacked together, aligned with guide-pins, and held together through boltholes at the corners. While this figure demonstrates only 4 layers, our lens has 11.

we have confirmed that the ASU Flexible Display Center is capable of manufacturing

III. EXPERIMENTAL SETUP

In order to test that the lens operates correctly, we performed a simple image-plane measurement. The physical setup for the experiment is shown in Fig. 3. To accomplish this, the transmitter (Tx) and receiver (Rx) were each placed 2 focal lengths away from the lens. We do this because placing the Tx $2f$ away from the lens causes its image to be $2f$ from the lens on the other side, as shown by the well-known lens equation:

$$\frac{1}{f} = \frac{1}{d_o} + \frac{1}{d_i} \quad (3)$$

Here, d_o is the distance of the object from the lens and d_i is the distance of the image from the lens. Thus, the receiver directly measures the image of the transmitter. In addition, the resultant absolute magnification of the image is 1.

The transmitter and receiver each consist of a K-band pyramidal horn antenna with nominal 14 dBi gain coupled to a WR-42 waveguide. The transmitter is fed by a signal generator emitting a 20 GHz tone at -20 dBm. The receiver was connected to a power meter. The power meter only nominally operates up to 18 GHz; however, we tested that the power meter responded linearly to power input at 20 GHz. Therefore, while the absolute measurements of the power meter were likely incorrect, we are confident in the relative power measurements that it provided.

Once the transmitter’s position was set, the receiver was scanned manually through the image plane until the point of maximum power reception was found. This was used as the zero-point for the measurement. The receiver was then manually moved up and down through the image plane in increments of a couple of millimeters. At each stopping point, the height of the receiver relative to its zero-point was

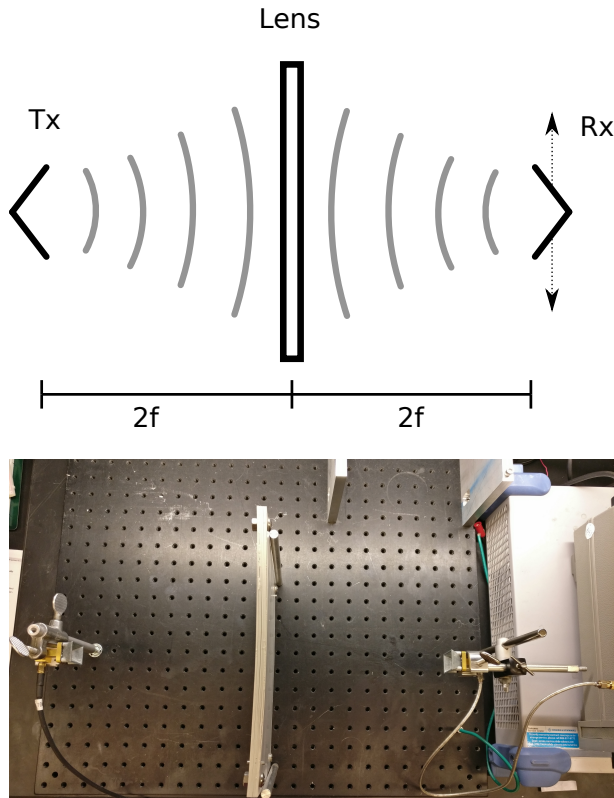


Fig. 3. A diagram of the test setup is display, with the realized setup displayed below it. The receiver and transmitter are both placed two focal lengths from the lens, such that the receiver sees an un-magnified image of the transmitter.

recorded, along with the power measurement from the power meter.

IV. ELECTROMAGNETIC SIMULATION

In order to further verify the accuracy of our lens design process, we have implemented an electromagnetic simulation which can propagate simulated beams. The simulation uses Fourier optics, implemented as described in Ref. [1].

We have demonstrated the ability of our simulation to handle lens beam transformations. In Fig. 4, we have plotted a simulation of the test setup described in the previous section. As we expected, we can see the beam diverge from the transmitter horn before being refocused to the receiver by the lens in the center.

We have not yet simulated the beam waist that we measured in our experiment and plotted in Fig. 5. However, in the future, this will serve as an important check that our design process works the way we think it does. It will also allow us to test the optical properties of our designs before we manufacture them.

V. RESULTS

Plotted with red circles in Fig. 5 is the result of the image plane measurement as described above. The magenta line is the best gaussian beam fit to the measurement.

Plotted in blue is what we would expect to measure if the lens were acting as an ideal lens. This was calculated

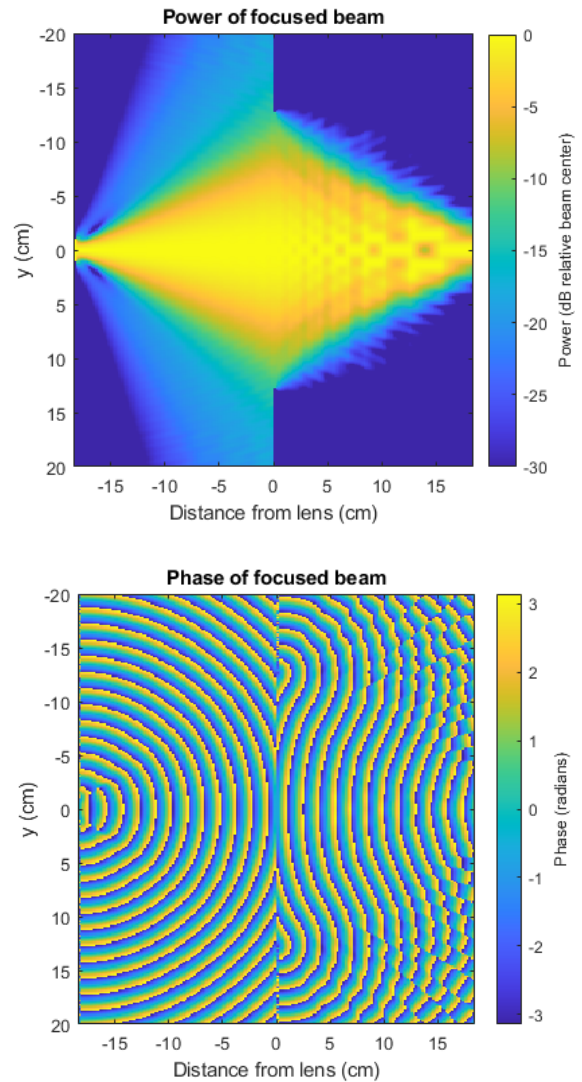


Fig. 4. Here is an electromagnetic simulation of our experimental test setup, plotted in magnitude and phase. On the left, the transmitter is emitting a roughly gaussian beam. On the right, the lens focuses the beam inward toward the receiver.

using the properties of the horn antennas, which we believe have beam waists of 8.4 mm at 20 GHz. By convolving the gaussian beam shapes of the two horns together, as described in Ref. [2], we expect the measured image to have an effective gaussian waist of approximately 11.9 mm.

The effective beam waist of the gaussian beam fit was 15.4 mm, which was about 30% wider than ideal. This indicates that the lens focuses properly, but does not focus as ideally as we expected it to. Future work will investigate the reasons for this non-ideal behaviour.

VI. CONCLUSION

We have successfully demonstrated the focusing abilities of our 20 GHz metamaterial flat lens. However, the gaussian beam focus is 30% wider than ideal.

Further testing would be necessary to determine whether this is due to manufacturer tolerance error, phase error in

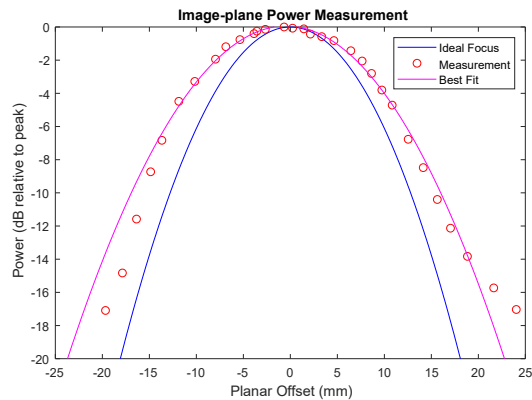


Fig. 5. Here is the plotted measurement of the image-plane scan compared to the expected beam measurement for an ideally focusing lens. The measured beam-width is about 30% wider than ideal.

the initial design, or an inaccurate estimate of the beam waists of the transmitter and receiver horns which were used. The simulation of the designed lens, which we are currently implementing, with its phase error included, could reveal whether or not the phase error was the cause. We also believe that a full near-field measurement of the lens would help to quantify the lens's performance in more meaningful ways.

In any case, we have demonstrated that our design process works well enough to accomplish an acceptable focus with our lens. We have also performed preliminary tests to demonstrate that our electromagnetic lens simulation is working as intended, which will help significantly in designing and testing future lenses. Using these results as a foundation, we will in future work scale the lens to higher frequencies. Doing so would allow their eventual application in CubeSat-based terahertz observations.

ACKNOWLEDGEMENTS

We would like to thank Rogers Corporation for providing us with RO3003 circuit board material free of charge, and the JPL SURP program for their financial support.

REFERENCES

- [1] Kristina K Davis, Willem Jellema, Stephen JC Yates, Christopher E Groppi, Jochem JA Baselmans, and Andrey Baryshev. Analysis techniques for complex field radiation pattern measurements. In *Millimeter, Submillimeter, and Far-Infrared Detectors and Instrumentation for Astronomy IX*, volume 10708, page 107082R. International Society for Optics and Photonics, 2018.
- [2] P.F. Goldsmith. *Quasioptical Systems: Gaussian Beam Quasioptical Propagation and Applications*. IEEE Press Series on RF and Microwave Technology. Wiley, 1998.
- [3] Eva Peral, Eastwood Im, Lauren Wye, Simon Lee, Simone Tanelli, Yahya Rahmat-Samii, Stephen Horst, Jim Hoffman, Sang-Ho Yun, Travis Imken, et al. Radar technologies for earth remote sensing from cubesat platforms. *Proceedings of the IEEE*, 106(3):404–418, 2018.
- [4] G Pisano, C Tucker, PA R Ade, P Moseley, and MW Ng. Metal mesh based metamaterials for millimetre wave and thz astronomy applications. In *Millimeter Waves and THz Technology Workshop (UCMMT), 2015 8th UK, Europe, China*, pages 1–4. IEEE, 2015.
- [5] Giampaolo Pisano, Ming Wah Ng, Fahri Ozturk, Bruno Maffei, and Vic Haynes. Dielectrically embedded flat mesh lens for millimeter waves applications. *Applied optics*, 52(11):2218–2225, 2013.

- [6] JM Rodriguez, Hristo D Hristov, and Walter Grote. Fresnel zone plate and ordinary lens antennas: Comparative study at microwave and terahertz frequencies. In *Microwave Conference (EuMC), 2011 41st European*, pages 894–897. IEEE, 2011.
- [7] David M Slocum, Thomas M Goyette, and Robert H Giles. High-resolution terahertz atmospheric water vapor continuum measurements. In *Terahertz Physics, Devices, and Systems VIII: Advanced Applications in Industry and Defense*, volume 9102, page 91020E. International Society for Optics and Photonics, 2014.